Journal of Molecular Catalysis B: Enzymatic 62 (2010) 230–234

Contents lists available at ScienceDirect

Journal of Molecular Catalysis B: Enzymatic

journal homepage: www.elsevier.com/locate/molcatb

Laboratory evolution of laccase for substrate specificity

Nirupama Gupta[a], Frederick S. Lee[a,b], Edgardo T. Farinas[a,*]

[a] Department of Chemistry and Environmental Science, New Jersey Institute of Technology, University Heights, Newark, NJ 07102, United States
[b] Chemistry–Physics Department, Kean University, 1000 Morris Avenue, Union, NJ 07083, United States

ARTICLE INFO

Article history:
Received 17 September 2009
Received in revised form 27 October 2009
Accepted 28 October 2009
Available online 10 November 2009

Keywords:
Directed evolution
Laccase
Substrate specificity
Thermal stability
Protein engineering

ABSTRACT

A laccase, CotA, from *Bacillus subtilis* was engineered using a combination of rational and directed evolution approaches. CotA is a generalist, an enzyme with broad specificity, and it was optimized to be a specialist, an enzyme with narrowed specificity. Wild-type CotA oxidizes ABTS (ABTS = diammonium 2,2′-azino-bis(3-ethylbenzothiazoline-6-sulfonate) and SGZ (SGZ = 4-hydroxy-3,5-dimethoxy-benzaldehyde azine), and it was engineered for increased specificity for ABTS. Based on the ABTS-bound crystal structure of CotA, 19 amino acids are within 6 Å of ABTS, and they were simultaneously randomized. A mutant was identified that was 132 times more specific for ABTS. Unexpectedly, the variant was found to acquire enhanced thermal stability. The half-life for the heat inactivation ($t_{1/2}$) at 80 °C was increased by 62 min for the mutant. Laccases have several applications in biotechnology, which include pulp bleaching, biosensors, bioremediation, and biofuel cells. The substrate specificity of CotA is moldable and the enzyme can be tailored to oxidize a variety of target molecules for specific purposes.

1. Introduction

Primitive cells were able to survive with a relatively small number of enzymes. Hence, ancient enzymes possessed broad substrate specificity that allowed them to perform several functions necessary for survival [1]. Eventually, gene duplication and mutation occurred, and enzymes developed into specialized roles as regulatory mechanisms emerged. In other words, a biocatalyst must be a generalist, an enzyme with broad specificity, before it can become a specialist, an enzyme with narrowed specificity.

Directed or laboratory evolution can mimic natural evolution on the bench top, and it is an effective tool for understanding these natural processes [2–5]. In addition, it is also a valuable method for protein engineering and elucidating fundamental structure/function relationships [6,7]. Engineering novel activity can occur through several routes, and one course is to create a generalist from the parent. Next, the generalist can be evolved into a specialist for the desired substrate. For example, beta-glucuronidase was evolved to hydrolyze beta-galactoside [8], and a mutant was found to be 500 times more efficient than the wild-type. The intermediate mutants before the final variant were shown to be generalists. These results support the hypothesis that enzymes acquire new function by diverging from an ancestor with broad specificity.

A suitable parent for novel activity should have broad substrate specificity and mutational robustness [3,4]. Mutational robustness is the protein's ability to undergo changes in the amino acid sequence and/or reaction conditions without disturbing function. Mutational robustness and thermal stability are closely related because proper structure should be retained for correct function. In short, a suitable parent for increased substrate specificity should be a generalist and thermostable.

Laccases [9] are members of the multicopper oxidase family of enzymes. They have diverse physiological roles such as lignin synthesis [10–12], lignin degradation [13,14], pathogenesis [15] and morphogenesis [16–20]. They catalyze the oxidation of a broad range of substrates, which include polyphenols, substituted phenols, diamines, and inorganic compounds [10,13]. Three structurally and functionally distinct copper centers are present. Initially, a one-electron oxidation of the reducing substrate occurs at the type-1 (T1) or blue copper center. The oxidation is coupled to a four-electron reduction of dioxygen to water, which takes place at a trinuclear copper cluster containing a type-2 (T2) and type-3 (T3) center. Laccases are attractive for many biotechnological applications such as pulp bleaching, biosensors for phenols, bioremediation, and the cathodic reactions in biofuel cells [15]. Furthermore, catalysis occurs with only substrate and dioxygen; therefore, there is no further requirement for additional electron transfer proteins or expensive cofactors.

Laccases are typically found in plants and fungi, and they are expressed as glycoproteins. Therefore, they are difficult to express and engineer in non-fungal expression systems [21]. Recently, bacterial laccases have been discovered [17]. Hence, high-throughput screening methods [22,23] can be used to study and design these enzymes [17,18]. CotA is a 65-kDa laccase, which is located on

* Corresponding author. Tel.: +1 973 642 7363; fax: +1 973 596 3586.
E-mail address: farinas@adm.njit.edu (E.T. Farinas).

1381-1177/$ – see front matter © 2009 Elsevier B.V. All rights reserved.
doi:10.1016/j.molcatb.2009.10.012

the outer coat of *Bacillus subtilis* spores. The role of CotA is not known, but it has been shown to be necessary for the biosynthesis of the brownish pigment characteristic of the spore [24]. The substrate-free and ABTS-bound (ABTS = diammonium 2,2′-azinobis(3-ethylbenzothiazoline-6-sulfonate) crystal structures of CotA [25,26] have been solved. The ABTS-bound structure is essentially identical to the native protein. The primary sequence of CotA has been aligned with known fungal laccase structures, and the copper-binding motifs and overall structure are similar [27]. Although the range of substrate diversity has not been comprehensively investigated, it is known that CotA catalyzes the oxidation of ABTS and SGZ (SGZ = 4-hydroxy-3,5-dimethoxy-benzaldehyde azine). Finally, CotA is a generalist and thermostable. Hence, it is suitable candidate for directed evolution.

The goal was to evolve CotA into specialist by increasing the substrate specificity for ABTS over SGZ. Previously, we described a suitable assay for substrate specificity [23]. A mutant, CotA-ABTS-1, was identified and characterized to be seven times more specific for ABTS. Guided by the ABTS-bound crystal structure, libraries were created by simultaneously randomizing the 19 amino acids that line the substrate-binding pocket. A mutant was identified that was 132 times more specific than the wild-type for ABTS. Unexpectedly, the variant was also found to acquire enhanced thermal stability. The heat inactivation of the variant at 80 °C was 62 min greater than the wild-type. This was surprising because this property was not included in the substrate specificity screen.

2. Materials and methods

2.1. Materials

All chemicals were of analytical reagent grade or higher quality and were purchased from Sigma–Aldrich (St. Louis, MO), Calbiochem (San Siego, CA), and Research Products International Corp. (Mt. Prospect, IL). Enzymes were purchased from Invitrogen (Carlsbad, CA) or New England Biolabs (Ipswich, MA). Primers were procured from Integrated DNA Technologies (Coralville, IA) or Eurofins MWG Operon (Huntswille, AL). DNA purifications kits were purchased from Qiagen (Valencia, CA).

2.2. Library creation

Saturation mutagenesis was performed on the 19 amino acids that line the substrate-binding pocket by following published procedures [23,28]. The four best clones (CotA-ABTS-1, CotA-ABTS-2, CotA-ABTS-3, and CotA-ABTS-4) identified from the saturation mutagenesis library were recombined following a published procedure [29]. A 50 μL reaction solution contained 5 μL of 10× PCR reaction buffer, $MgCl_2$ (1.5 mM), dNTPs (0.2 mM), *taq* DNA polymerase (2.5 unit), forward primer (30 pmol; 5′-GCGCTAGCAGGAGGAATTCACCATGACACTTGAA-3′), reverse primer (30 pmol; 5′-GCGCAAGCTTTTATTTATGGGGATCAGTTAT-3′), and 10 ng of each template. The PCR program consisted of 100 cycles at 94 °C for 30 s, 55 °C for 5 s, and 56 °C for 5 s. The PCR product was diluted 10-fold in a 100 μL reaction containing 10 μL of 10× PCR reaction buffer, $MgCl_2$ (1.5 mM), dNTPs (0.2 mM), *Pfu* DNA polymerase (1 unit), forward primer (0.5 μM) and reverse primer (0.5 μM). The PCR program consisted of 30 cycles at 95 °C for 30 s, 55 °C for 30 s, and 72 °C for 3 min. The recombination library was screened following published procedures [23].

2.3. Kinetics measurements

Sequences were verified using ABI BigDye Terminator chemistry on an ABI 3130xl Genetic Analyzer (Molecular Resource Facility, University of Medicine and Dentistry of New Jersey, Newark). Expression and purification of the CotA mutants were performed by following literature procedures [23]. Each clone was expressed at least two times, and for each expression and purification, the measurements were done in triplicate.

The kinetic parameters of purified laccases were determined at 25 °C by using ABTS (1–100 μM) in sodium acetate (100 mM, pH 4) buffer or SGZ (1–150 μM) in potassium phosphate (100 mM, pH 6) buffer. The reactions were initiated by adding between 0.01 and 6.0 μg enzyme. The initial rates were acquired from the linear portion of the reaction curve. Kinetic parameters were obtained by curve fitting (SigmaPlot 10.0, Systat Software Inc., San Jose, CA).

2.4. Thermal inactivation

The half-lives of thermal inactivation ($t_{1/2}$) of wild-type CotA and the mutants were determined by measuring the residual activity. The enzyme (10 μg/mL) was incubated in Tris–HCl buffer (20 mM, pH 7.6) at 80 °C. 10 μL samples were drawn every 20 min and diluted into 120 μL acetate buffer (100 mM, pH 4.0). The resulting solutions were equilibrated to 25 °C. The reaction was initiated by adding ABTS (1.0 mM), and the activity was monitored at 420 nm.

2.5. Protein modeling and molecular dynamic simulations

All protein modeling and molecular dynamic simulations described in this work were carried out using the commercial software MOE (Chemical Computing Group, Montreal, Canada).

The three-dimensional (3D) models of the two point mutants (G417L and L386W) and the double mutant (G417L:L386W) were constructed based on the wild-type (WT) co-crystal structure of CotA and ABTS (PDB accession code 1UVW). First, wild-type side chains in question were replaced by the corresponding mutant side-chain rotamers. Then the raw mutant models were energy-minimized to remove bad van der Waals contacts to generate the working mutant models.

Energy minimizations (EM) were performed by using the MMFF94x [30–32] force field along with the default minimization parameters in MOE that included an 8 Å cutoff for the non-bonded interaction. Implicit solvation, which is described by the Generalized Born model, was used instead of the default Distance-dependent model. In addition, all heavy atoms were harmonically constrained to their initial coordinates with a force constant of 100 kcal/mol during EM.

Molecular dynamic (MD) simulations at 300 K were carried out by using identical force field potentials as in EM except that heavy atoms were tethered to their starting coordinates with a force constant of 0.1 kcal/mol. Default MD parameters in MOE were used except that all bonds were constrained during the simulations. The MD time steps were 2 fs.

3. Results and discussion

Laccases are typically found in plants and fungi as glycoproteins [18], and they are poorly expressed in non-fungal protein expression systems, which makes them difficult to engineer [33–35]. Hence, laccase optimization has been hindered using directed evolution methods. Recently, laccases have been discovered in prokaryotes. Hence, high-throughput screening methods can be used to tune these enzymes [22,23].

Laccases catalyze the oxidation for a broad range of substrates. A combination of directed evolution and structure-based methods is used to improve the substrate specificity. The ABTS-CotA structure [25,26] displays that 23 amino acids (Pro226, Ala227, Phe228, Cys229, Thr260, Arg261, Thr262, Gly321, Cys322, Gly323, Gly324, Gln378, Gly382, Pro384, Leu386, Thr415, Arg416, Gly417, Thr418,

Table 1
Kinetic parameters for wild-type CotA and mutants.

Enzyme	ABTS		k_{cat}/K_M (s^{-1} μM^{-1})	SGZ		k_{cat}/K_M (s^{-1} μM^{-1})	$(k_{cat}/K_m)_{ATBS}/(k_{cat}/K_m)_{SGZ}$
	k_{cat} (s^{-1})	K_M (μM)		k_{cat} (s^{-1})	K_M (μM)		
WT-CotA	293.3 ± 9.0	32.5 ± 2.3	9.1	169.0 ± 2.8	37.0 ± 2	4.5	2.0
CotA-ABTS-1	639.6 ± 16.0	21.0 ± 3.2	30.4	78.0 ± 6	35.0 ± 4.0	2.1	13.9
CotA-ABTS-3	500.0 ± 18.0	58.0 ± 6.0	8.6	86 ± 7.0	77.0 ± 5.0	1.1	7.8
CotA-ABTS-10	636.0 ± 9.0	9.6 ± 1.6	66.0	21.0 ± 2.0	84.0 ± 9.0	0.25	264.0

His419, Ile494, His497, and Met502) are within 6 Å of the substrate. His419, His497, and Cys492 chelate the copper T1 site and Cys229 and Cys322 form a disulfide bond. Hence, these amino acids were not included in the randomization. A total of 19 amino acids were randomized. A mutation rate was previously estimated for various saturation mutagenesis libraries [23], and a library was chosen to have between one and two amino acid substitutions per gene in order to keep the library size manageable.

Positive clones were chosen that exhibited at least 1.5 times the mean value of the wild-type ABTS:SGZ endpoint absorbance ratio [36]. A higher value would indicate that the mutant is more specific for ABTS. The first round of screening identified eight clones (CotA-ABTS-1–8). These clones were rescreened for the ABTS:SGZ absorbance ratios and initial rates. CotA-ABTS-1, CotA-ABTS-2, CotA-ABTS-3 and CotA-ABTS-4 were more active and possessed an ABTS:SGZ absorbance ratio at least 1.5-fold greater than wild-type. The mutants were sequenced, which revealed single point mutations for CotA-ABTS-1 (Gly417Leu), CotA-ABTS-3 (Leu386Trp), and CotA-ABTS-4 (Leu386Ile). A double mutation was found for CotA-ABTS-2 (Gly321Arg and Gln378Ser). On the other hand, CotA-ABTS-5, CotA-ABTS-6, CotA-ABTS-7 and CotA-ABTS-8 were also more specific for ABTS, but the initial rates were lower than the wild-type. Hence, these clones were not pursued further.

CotA-ABTS-1, CotA-ABTS-2, CotA-ABTS-3 and CotA-ABTS-4 were recombined by the staggered extension process [29]. The library was screened, and four mutants were identified with increased substrate specificity. The sequences of two clones were identical to CotA-ABTS-1, and the other two were mutants, CotA-ABTS-9 (Gly417Leu and Gln378Ser) and CotA-ABTS-10 (Gly417Leu and Leu386Trp). Both mutants acquired the Gly417Leu mutation from CotA-ABTS-1. The other mutation for CotA-ABTS-9 and CotA-ABTS-10 originated from CotA-ABTS-2 and CotA-ABTS-3, respectively. Next, CotA-ABTS-9 and CotA-ABTS-10 were rescreened. The total activity for both mutants was within 10% of CotA-ABTS-1 for ABTS, and the ABTS:SGZ absorbance ratio was 3.5 and 6.0 for CotA-ABTS-9 and CotA-ABTS-10, respectively. Hence, the best mutant, CotA-ABTS-10, was chosen for purification, kinetic analysis, protein modeling and molecular dynamic simulation.

The kinetic parameters were determined for wild-type CotA, CotA-ABTS-1, CotA-ABTS-3, and CotA-ABTS-10 (Table 1) in triplicate for two separate protein expressions (Fig. 1). The $(k_{cat}/K_M)_{ABTS}/(k_{cat}/K_M)_{SGZ's}$, for wild-type CotA and CotA-ABTS-10 were 2.0 and 264, respectively. Therefore, CotA-ABTS-10 is 132 times more specific, $[(k_{cat}/K_M)_{ATBS}/(k_{cat}/K_M)_{SGZ}]_{CotA\text{-}ABTS\text{-}10}/[(k_{cat}/K_M)_{ATBS}/(k_{cat}/K_M)_{SGZ}]_{wild\text{-}type\ CotA}$, for ABTS than the wild-type. CotA-ABTS-1 and CotA-ABTS-3, the parents for CotA-ABTS-10, were 7.0 and 3.9 times more specific, respectively.

The K_M of CotA-ABTS-1 for ABTS decreased from 32.5 μM to 21.0 μM, and the k_{cat} increased from 293.3 s^{-1} to 639.6 s^{-1}. The 3D model of the point mutant Gly417Leu shows that the Leu417 side chain may provide favorable van der Waals interactions with the ethyl group of the benzothiazole ring (Fig. 2A). This may account for the decrease in K_M. On the other hand, the ethyl group is absent in SGZ and the K_M's are similar for wild-type CotA and CotA-ABTS-1. The k_{cat} for the CotA-ABTS-1 is approximately double for ABTS and half for SGZ. The rate-limiting step has been proposed to be substrate oxidation [37,38]. The thiaxoline ring of ABTS is perpendicular and 3.32 Å from His497 [25], which is ligated to the T1-copper center. This arrangement permits a favorable arrangement for electron transfer to the blue copper center. The substrate specificity is primarily due to an increase in k_{cat} for ABTS, which may be due to optimizing the substrate geometry. This helps to explain the differential selectivity of the Gly417Leu variant towards ABTS over SGZ.

CotA-ABTS-3 is 3.9-fold more specific for ABTS than the wild-type. The k_{cat} values for ABTS and SGZ are 500.0 s^{-1} and 86.0 s^{-1}, and the K_M values are 58.0 μM and 77.0 μM, respectively. The 3D model of the mutant (Fig. 2B) shows that the indole N–H of Trp386 is positioned within hydrogen bond distances (2.94 Å) and angles (150°) to the azino nitrogens of ABTS (Fig. 2B). However, the mutant K_M is nearly double than the wild-type. Hence, it is unlikely that an H-bond is being formed. The substrate specificity is due to an increase in k_{cat} for ABTS and the overall decrease in k_{cat}/K_M for SGZ.

CotA-ABTS-10 resulted from the recombination of CotA-ABTS-1 and CotA-ABTS-3. The k_{cat}'s of CotA-ABTS-10 for ABTS and SGZ are 636.0 s^{-1} and 21.0 s^{-1}, and the K_M's are 9.6 μM and 84.0 μM,

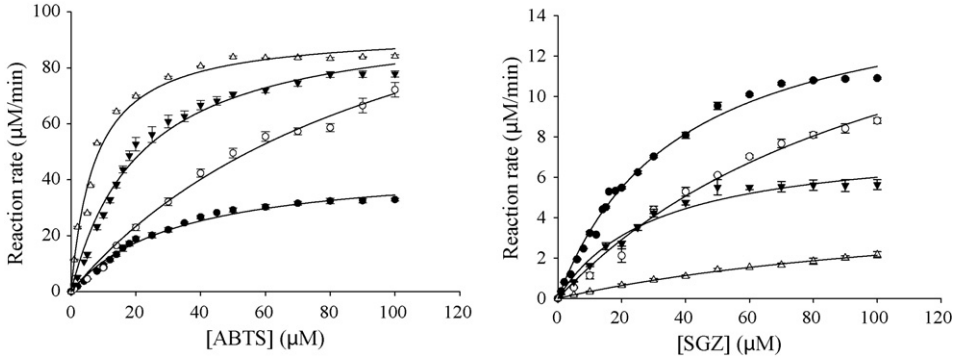

Fig. 1. Kinetic analysis for wild-type CotA and variants. (A) Wild-type CotA (closed circle), CotA-ABTS-1 (closed inverted triangle), CotA-ABTS-3 (open circle), and CotA-ABTS-10 (open triangle) reaction rates are plotted against ABTS concentration. (B) Wild-type CotA (closed circle), CotA-ABTS-1 (closed inverted triangle), CotA-ABTS-3 (open circle), and CotA-ABTS-10 (open triangle) reaction rates are plotted against SGZ concentration.

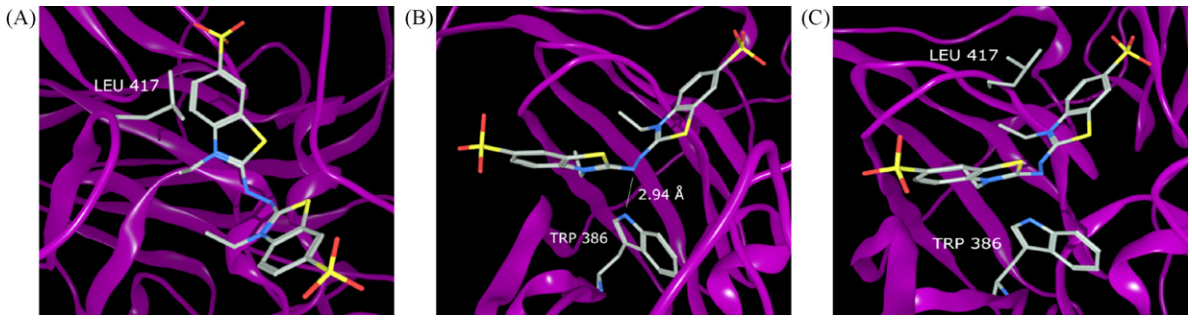

Fig. 2. Computer models of ABTS-CotA variants with protein backbones depicted as ribbons. (A) The 3D model of CotA-ABTS-1 (G417L) suggests direct contact between the side chain of L417 and ABTS. (B) The 3D model of CotA-ABTS-3 (L386W) suggests that the indole nitrogen is within H-bond distances (~3 Å) and angles (~150°) to the two azino nitrogens of ABTS. (C) The 3D model of the double mutant CotA-ABTS-10 (G417L and L386W) shows how ABTS is sandwiched by the two mutations.

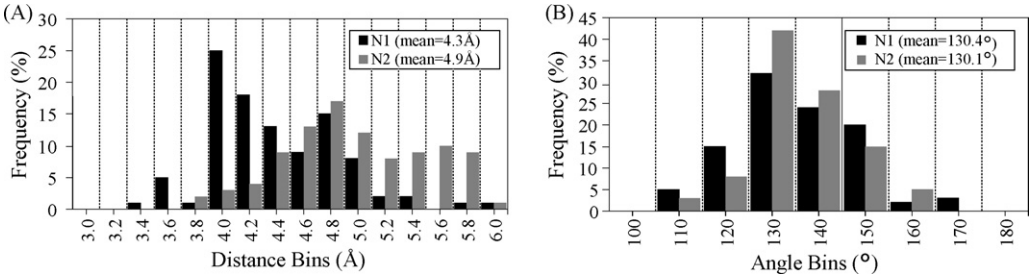

Fig. 3. Distance and angle distributions of the H-bond in question of CotA-ABTS-10 as studied by molecular dynamics at 300 K. The H-bond in question is between the indole N–H of W386 and either azino nitrogen of ABTS. (A) Distance distribution of the H-bond in question during the 1 ns MD simulation. (B) Angle distribution of the same H-bond during the MD simulation.

respectively. CotA-ABTS-10 is 132-fold more specific than the wild-type (Fig. 2). The Leu and Typ mutations sandwich ABTS (Fig. 2C). In light of the experimental results for CotA-ABTS-3, the improvements in K_M of the double mutant for ABTS are likely not due to the previously mentioned H-bond interaction from modeling. Instead, favorable hydrophobic interactions are more likely responsible for the enhanced substrate binding. To substantiate this claim, the feasibility of an H-bond between the double mutant (Fig. 2C) and ABTS was investigated in a 1 ns MD simulation with Generalized Born solvation at 300 K. The distributions of H-bond distances and angles between the indol N–H and the two azino nitrogens of ABTS (referred to as N1 and N2) were shown in Fig. 3. The mean distance and angle of the shorter H-bond were found to be 4.3 ± 0.5 Å and $130.4 \pm 12.6^\circ$, respectively. This indicated that the H-bond in question became far less favorable when the mutant–substrate complex was equilibrated at 300 K.

The thermal inactivation of wild-type CotA and the mutants was determined by measuring the residual activity. The enzymes were incubated at 80 °C for a specified amount of time, and the half-lives of heat inactivation ($t_{1/2}$) were determined following first-order kinetics (inset in Fig. 4). The $t_{1/2}$'s were 113 min ($k = 0.00611\ \text{min}^{-1}$), 175 min ($k = 0.00394\ \text{min}^{-1}$), 150 min ($k = 0.00462\ \text{min}^{-1}$), and 175 min ($k = 0.00395\ \text{min}^{-1}$) for wild-type CotA, CotA-ABTS-1, CotA-ABTS-3, and CotA-ABTS-10, respectively (Fig. 4).

The wild-type was already thermostable, and $t_{1/2}$ at 80 °C is 113 min. Most remarkable is that the $t_{1/2}$ for CotA-ABTS-10 is 175 min. This is unexpected because thermal stability was not included in the substrate specificity assay. In general, protein stability should decrease as the number of mutations increase. Furthermore, laboratory evolution for substrate specificity is normally not coupled to increased thermal stability [39].

Wild-type CotA is able to accept several substrates, which is presumably due to plasticity of the substrate-binding pocket. Hence, mutations may stabilize the correct structural conformation for ABTS at the expense of SGZ. For example, glycine is known to allow for greater conformational flexibility, and the leucine substitution

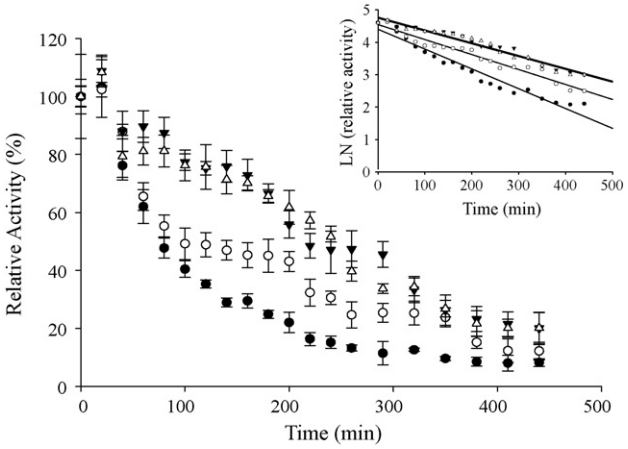

Fig. 4. Half-life for heat inactivation ($t_{1/2}$) of wild-type CotA and mutants. Wild-type CotA (closed circle), CotA-ABTS-1 (closed inverted triangle), CotA-ABTS-3 (open circle), and CotA-ABTS-10 (open triangle) residual activity at 80 °C is plotted against time. The inset represents the first-order kinetics of deactivation.

may induce stabilizing secondary structure. Next, the thermal stability may also be due to the assay conditions. The cell lysates used in the screen were incubated at 37 °C at 30 min with DNaseI and lysozyme. Furthermore, the lysates did not contain protease inhibitors to prevent protein digestion. This situation would favor mutants resistant to protease degradation, which would result in isolating more stable mutants. However, it is difficult to ascertain the origin of the thermal stability without a detailed thermodynamic and structural investigation.

4. Conclusions

CotA oxidizes a range of substrates and it is able to tolerate mutations. These attributes are desirable for a successful directed

evolution experiment. Structural information and directed evolution methods were combined to efficiently optimize CotA for ABTS oxidation over SGZ. The substrate-binding pocket contains a high degree of plasticity, and it can be tailored for a number of biotechnological applications. For example, laccases have been used for paper bleaching using mediators such as ABTS. Hence, CotA-ABTS-10 may be more effective for this purpose. Surprisingly, the mutant gained thermal stability, and this feature was not included in the screen. Additional research must be explored to identify the connection between substrate specificity and thermal stability.

Acknowledgement

This research was partially supported by the National Science Foundation (MCB-0746078).

References

[1] R.A. Jensen, Annu. Rev. Microbiol. 30 (1976) 409–425.
[2] O. Khersonsky, C. Roodveldt, D.S. Tawfik, Curr. Opin. Chem. Biol. 10 (2006) 498–508.
[3] C.A. Tracewell, F.H. Arnold, Curr. Opin. Chem. Biol. 13 (2009) 3–9.
[4] T.L. O'Loughlin, W.M. Patrick, I. Matsumura, Protein Eng. Des. Select. 19 (2006) 439–442.
[5] A. Aharoni, L. Gaidukov, O. Khersonsky, Q.G.S. Mc, C. Roodveldt, D.S. Tawfik, Nat. Genet. 37 (2005) 73–76.
[6] F.H. Arnold, Advances in Protein Chemistry, Academic Press, New York, 2001.
[7] E.T. Farinas, T. Bulter, F.H. Arnold, Curr. Opin. Biotechnol. 12 (2001) 545–551.
[8] I. Matsumura, A.D. Ellington, J. Mol. Biol. 305 (2001) 331–339.
[9] E.I. Solomon, U.M. Sundaram, T.E. Machonkin, Chem. Rev. 96 (1996) 2563–2606.
[10] W. Boa, D.M. O'Malley, R. Whetten, R.R. Sederoff, Science 260 (1993) 672–674.
[11] A. Huttermann, C. Mai, A. Kharazipour, Appl. Microbiol. Biotechnol. 55 (2001) 387–394.
[12] B.C. McCaig, R.B. Meagher, J.F. Dean, Planta 221 (2005) 619–636.
[13] D. Rochefort, R. Bourbonnais, D. Leech, M.G. Paice, Chem. Commun. (2002) 1182–1183.
[14] D. Rochefort, D. Leech, R. Bourbonnais, Green Chem. 6 (2004) 14–24.
[15] A.M. Mayer, R.C. Staples, Phytochemistry 60 (2002) 551–565.
[16] S. Chen, W. Ge, J.A. Buswell, FEMS Microbiol. Lett. 230 (2004) 171–176.
[17] H. Claus, Arch. Microbiol. 179 (2003) 145–150.
[18] H. Claus, Micron 35 (2004) 93–96.
[19] N.T. Dittmer, R.J. Suderman, H. Jiang, Y.C. Zhu, M.J. Gorman, K.J. Kramer, M.R. Kanost, Insect Biochem. Mol. Biol. 34 (2004) 29–41.
[20] J. Zhao, H.S. Kwan, Appl. Environ. Microbiol. 65 (1999) 4908–4913.
[21] T. Bulter, M. Alcalde, V. Sieber, P. Meinhold, C. Schlachtbauer, F.H. Arnold, Appl. Environ. Microbiol. 69 (2003) 987–995.
[22] V. Brissos, L. Pereira, F.D. Munteanu, A. Cavaco-Paulo, L.O. Martins, Biotechnol. J. 4 (2009) 558–563.
[23] N. Gupta, E.T. Farinas, Comb. Chem. High Throughput Screen. 12 (2009) 269–274.
[24] M.F. Hullo, I. Moszer, A. Danchin, I. Martin-Verstraete, J. Bacteriol. 183 (2001) 5426–5430.
[25] F.J. Enguita, D. Marcal, L.O. Martins, R. Grenha, A.O. Henriques, P.F. Lindley, M.A. Carrondo, J. Biol. Chem. 279 (2004) 23472–23476.
[26] F.J. Enguita, L.O. Martins, A.O. Henriques, M.A. Carrondo, J. Biol. Chem. 278 (2003) 19416–19425.
[27] L.O. Martins, C.M. Soares, M.M. Pereira, M. Teixeira, T. Costa, G.H. Jones, A.O. Henriques, J. Biol. Chem. 277 (2002) 18849–18859.
[28] W.P. Stemmer, A. Crameri, K.D. Ha, T.M. Brennan, H.L. Heyneker, Gene 164 (1995) 49–53.
[29] H. Zhao, L. Giver, Z. Shao, J.A. Affholter, F.H. Arnold, Nat. Biotechnol. 16 (1998) 258–261.
[30] M.C. Orencia, M.A. Hanson, R.C. Stevens, Adv. Protein Chem. 55 (2001) 227–259.
[31] T.A. Halgren, J. Comput. Chem. 20 (1999) 720–729.
[32] T.A. Halgren, J. Comput. Chem. 20 (1999) 730–748.
[33] M. Alcalde, T. Bulter, M. Zumarraga, H. Garcia-Arellano, M. Mencia, F.J. Plou, A. Ballesteros, J. Biomol. Screen. 10 (2005) 624.
[34] M. Zumarraga, T. Bulter, S. Shleev, J. Polaina, A. Martinez-Arias, F.J. Plou, A. Ballesteros, M. Alcalde, Chem. Biol. 14 (2007) 1052.
[35] M. Zumarraga, S. Camarero, S. Shleev, A. Martinez-Arias, A. Ballesteros, F.J. Plou, M. Alcalde, Protein: Struct. Funct. Gen. 71 (2008) 250–260.
[36] O. Salazar, L. Sun, in: F.H. Arnold, G. Georgiou (Eds.), Directed Enzyme Evolution: Screening and Selection Methods, Humana Press, Totowa, 2003, pp. 85–97.
[37] F. Xu, Biochemistry 35 (1996) 7608–7614.
[38] F. Xu, W. Shin, S.H. Brown, J.A. Wahleithner, U.M. Sundaram, E.I. Solomon, Biochim. Biophys. Acta 1292 (1996) 303–311.
[39] F.H. Arnold, Acc. Chem. Res. 31 (1998) 125–131.